

Transaminase - carbonic anhydrase bi-enzymatic cascade for preparation of (*R*)-1-arylethan-1-amines and (*S*)-1-arylethan-1-ols

Laura Edit Barabás,^a Diana Maria Scrob,^a Andrea Varga,^a Loránd Kiss^b, Monica Ioana Toşa,^a Csaba Paizs^{a*}

^aBabeş-Bolyai University, Enzymology and Applied Biocatalysis Research Center, Arany János 11, Cluj-Napoca, 400028-România

^bInstitute of Organic Chemistry, Stereochemistry Research Group, Research Centre for Natural Sciences, H-1117 Budapest, Magyar Tudósok krt. 2, Hungary

*Correspondence: csaba.paizs@ubbcluj.ro;

Table of Contents

S1. Materials and methods	1
S2. Transformation of plasmids DNA into <i>E. coli</i>	1
S3. Protein purification	2
S3.1. SDS-PAGE analysis	2
S4. DMSO tolerance of hCAII – melting temperature measurements	2
S5. HPLC separation methods	3
S5.1. HPLC separation methods to determine the conversions of transamination reactions	3
S5.2. HPLC separation method to determine the enantiomeric excess (<i>ee</i>) of (<i>S</i>)-3a-d	3
S5.3. HPLC separation method to determine the conversion of the reduction reaction of 2a	3
S6. HPLC calibration procedure of 2a and (<i>S</i>)-3a	4
S7. Chromatographic monitoring of biocatalytic reactions	4
S8. Effect of cosolvent content on the catalytic performance of hCAII	18
S9. Cellular biotransformation	19

S1. Materials and methods

The commercial chemicals and solvents used in our experiments were products of Sigma-Aldrich or Alfa Aesar. LB medium was purchased from Liofilchem (Roseto, Italy), protease inhibitor cocktail from Hoffmann–La Roche (Basel, Switzerland), while the Ni-NTA Superflow resin used for affinity chromatography was from Qiagen (Hilden, Germany). Nano differential scanning fluorimetry (nanoDSF) measurements were performed using Prometheus NT.48 instrument (NanoTemper Technologies, München, Germany). The high performance liquid chromatography (HPLC) measurements were conducted with Agilent 1200 and 1100 Series systems (Santa Clara, CA, USA).

S2. Transformation of plasmids DNA into *E. coli*

Transformations of hCAII-pET-28a(+) and *PpS*-TA-pET-19b plasmids DNA into *E. coli* BL21 (DE3) pLysS Gold and *E. coli* BL21 GOLD (DE3) were performed using the electroporation method. After thawing the electrocompetent bacterial cells (50 µL) on ice for 20 min, 1 µL of plasmid DNA was added, followed by incubation on ice for 1 min. After that, the electrocompetent cells containing the plasmid were transferred into a prechilled electroporation cuvette and pulsed twice with 1800V; 300 µL of SOC (Super Optimal broth with Catabolite repression) medium was added quickly to the cuvette, mixed gently, and transferred into a microcentrifuge tube followed by incubation at 37 °C for 1 h with shaking.

The transformed bacteria were plated on Luria-Bertani (LB) agar plates supplemented with kanamycin (25 µg mL⁻¹) and chloramphenicol (30 µg mL⁻¹) - in the case of transformation of hCAII, and with carbenicillin (50 µg mL⁻¹) and chloramphenicol (30 µg mL⁻¹) - in the case of *PpS*-TA. Agar plates were incubated overnight at 37 °C, forming single colonies of bacteria bearing the plasmids encoding the recombinant protein.

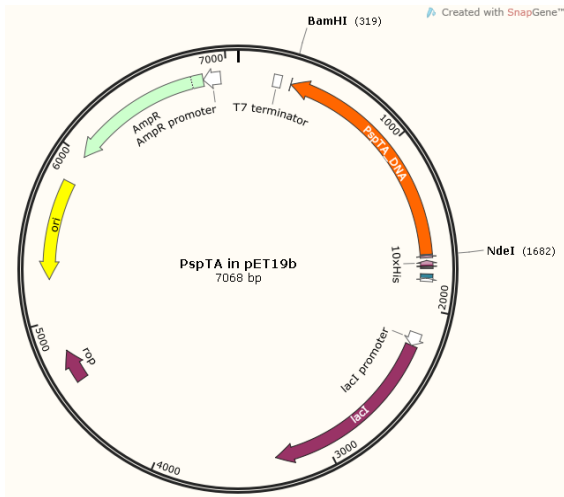


Fig. S1. The *Pps*-TA gene in the expression vector

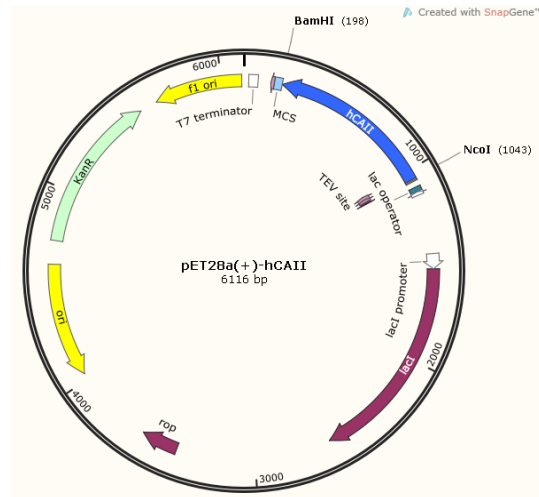


Fig. S2. The hCAII gene in the expression vector

S3. Protein purification

See the Main Text for the purification protocol.

S3.1. SDS-PAGE analysis

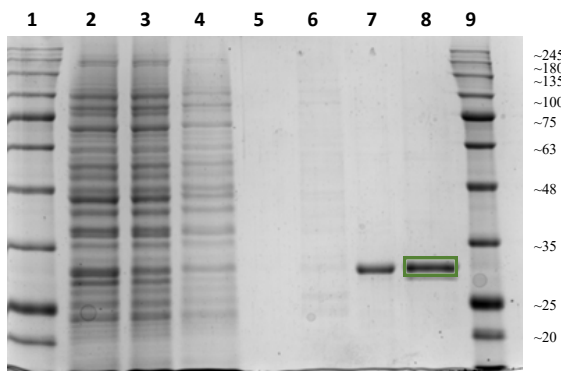


Fig. S3. SDS-PAGE analysis performed on a 12% gel for the purification of the recombinant hCAII on Ni-NTA column. **1:** protein marker, **2:** supernatant of the lysated cell, **3:** flow-through, **4:** washing with low salt buffer solution (LS solution: 50 mM TRIS, 30 mM KCl, pH 8.0), **5:** washing with high salt buffer solution (HS solution: 50 mM TRIS, 300 mM KCl, pH 8.0), **6:** washing with 25 mM imidazole (25 mM imidazole solution in LS), **7:** hCAII eluted with 300 mM imidazole, **8:** hCAII after dialysis (~32 kDa), **9:** protein marker

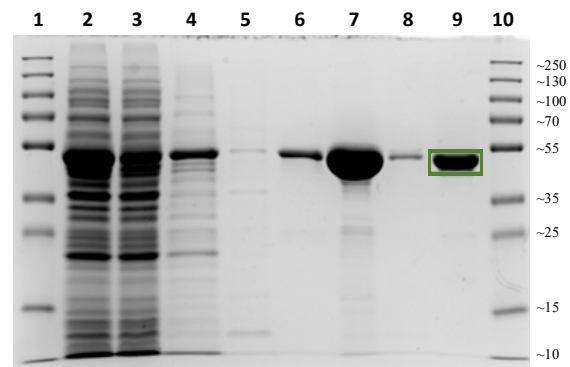


Fig. S4. SDS-PAGE analysis performed on a 12% gel for the purification of the recombinant *Pps*-TA on Ni-NTA column. **1:** protein marker, **2:** supernatant of the lysated cell, **3:** flow-through, **4:** washing with low salt buffer solution (LS solution: 50 mM HEPES, 30 mM KCl, pH 7.0), **5:** washing with high salt buffer solution (HS solution: 50 mM HEPES, 300 mM KCl, pH 7.0), **6:** washing with 10 mM imidazole (10 mM imidazole solution in LS), **7:** *Pps*-TA eluted with 300 mM imidazole, **8:** 1 M imidazole, **9:** *Pps*-TA after dialysis (~50 kDa), **10:** protein marker

S4. DMSO tolerance of hCAII – melting temperature measurements

The melting temperatures of the protein solutions were determined by nanoDSF technology using a Prometheus NT.48 (*NanoTemper Technologies*, München, Germany) instrument. The nanoDSF grade standard capillaries were filled with enzyme solution in TRIS (50 mM, pH 8.0) buffer, which contained 0-50 % DMSO (v/v). These samples were heated from 20 °C to 70 °C and the thermal ramping rate was 1 °C min⁻¹.

S5. HPLC separation methods

S5.1. HPLC separation methods to determine the conversions of transamination reactions

With the aim to determine the conversions of the kinetic resolution reactions, samples were prepared by taking 5-40 μL (depending on the substrate concentration) from the reaction mixture; 300 μL of methanol was added to stop the reaction and dilute the sample. The samples were centrifuged at 13000 rpm (5 min) using a 0.22 μm nylon membrane filter. After centrifugation 300 μL HClO_4 (pH 1.0) was added to the sample and it was injected into HPLC (Agilent 1100 Series) using the following analytical column: Daicel CROWNPAK® CR-I(+), 3 \times 150 mm, 5 μm .

Table S1. Chiral separation methods for racemic amines (\pm)-1a-d

Compounds	Eluent HClO_4 (pH 1):ACN	Flow rate (mL min^{-1})	Temp. ($^\circ\text{C}$)	Retention time (min)		
				Ketone	Amine	
					(S)	(R)
(\pm)-1a	60:40	0.4	25	4.4	5.8	8.7
(\pm)-1b	40:60	0.4	15	3.5	4.7	7.7
(\pm)-1c	50:50	0.4	25	3.9	5.1	7.5
(\pm)-1d	50:50	0.4	25	4.9	5.5	8.6

S5.2. HPLC separation method to determine the enantiomeric excess (*ee*) of (S)-3a-d

A normal-phase HPLC method was used for the chiral separation of the enantiomers using a CHIRALPAK AS-H 4.6 \times 250 mm column. A volume of 1 mL of reaction mixture was extracted with hexane-ethyl acetate (1:3, v/v, three times). The combined organic layer was dried over anhydrous Na_2SO_4 , and the solvent was removed using TurboVap evaporator. The product mixture was dissolved in the eluent mixture (*n*-hexane-2-propanol) and injected into the HPLC (Agilent 1200 Series). A detailed description of the HPLC separation methods can be found in **Table S2**.

Table S2. Chiral separation methods of racemic 1-phenylethanols and corresponding ketones

Compounds	Eluent ^a <i>n</i> -hexane:2-propanol	Retention time (min)		
		Ketone	Alcohol	
			(R)	(S)
3a	97:3	8.1	10.9	12
3b	98:2	11.3	19.7	21.6
3c	93:7	9.6	11.5	14.7
3d	97:3	11.9	21.9	24.1

^a 1 mL min^{-1} flow rate and 10 $^\circ\text{C}$

S5.3. HPLC separation method to determine the conversion of the reduction reaction of 2a

A simple and rapid separation method was developed to monitor the conversions using ZORBAX Eclipse XDB-C8, 4.6 \times 150 mm, 5 μm column. The mobile phase composition was 35 % H_2O and 65 % acetonitrile. The flow rate was 1 mL min^{-1} and the column thermostat was set to 25 $^\circ\text{C}$.

The samples were prepared by taking 20-50 μL (depending on the substrate concentration) from the reaction mixture; 300 μL of methanol was added to stop the reaction and dilute the sample. The samples were centrifuged at 13000 rpm (5 min) using a 0.22 μm nylon membrane filter. After centrifugation 300 μL H_2O was added to the sample and it was injected into HPLC (Agilent 1100 Series) using the previous method.

S6. HPLC calibration procedure of 2a and (S)-3a

The calibration curve shown in Fig. S5. was used to determine the response factor between the signals produced by the substrate 2a and the product (S)-3a of the enzymatic reduction reaction, at 210 nm wavelength.

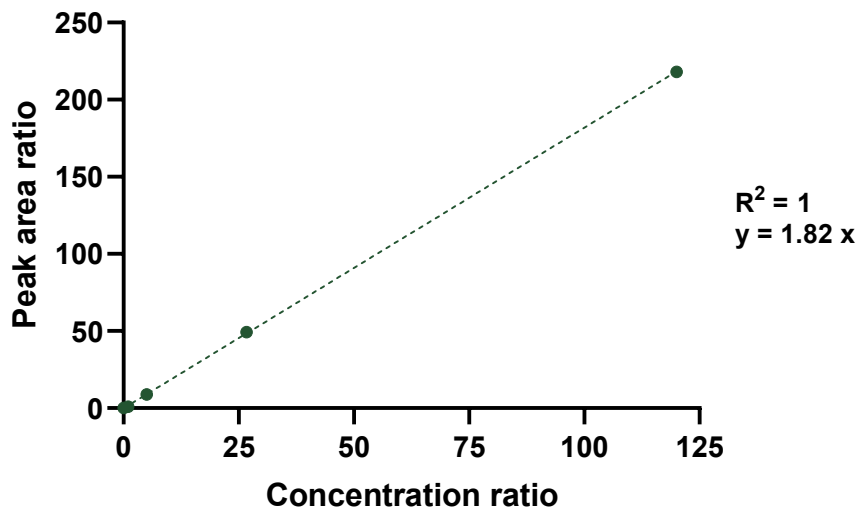


Fig. S5. Calibration curve of 2a and 3a

S7. Chromatographic monitoring of biocatalytic reactions

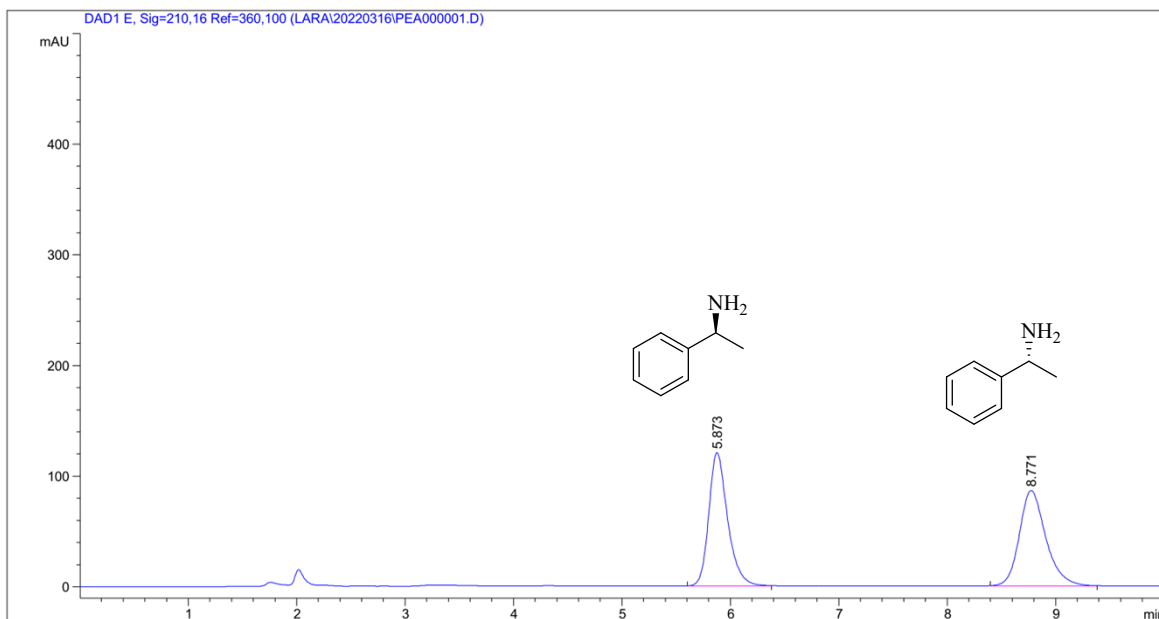


Fig. S6. Chiral separation of (±)-1a on Crownpak CR-I(+)column

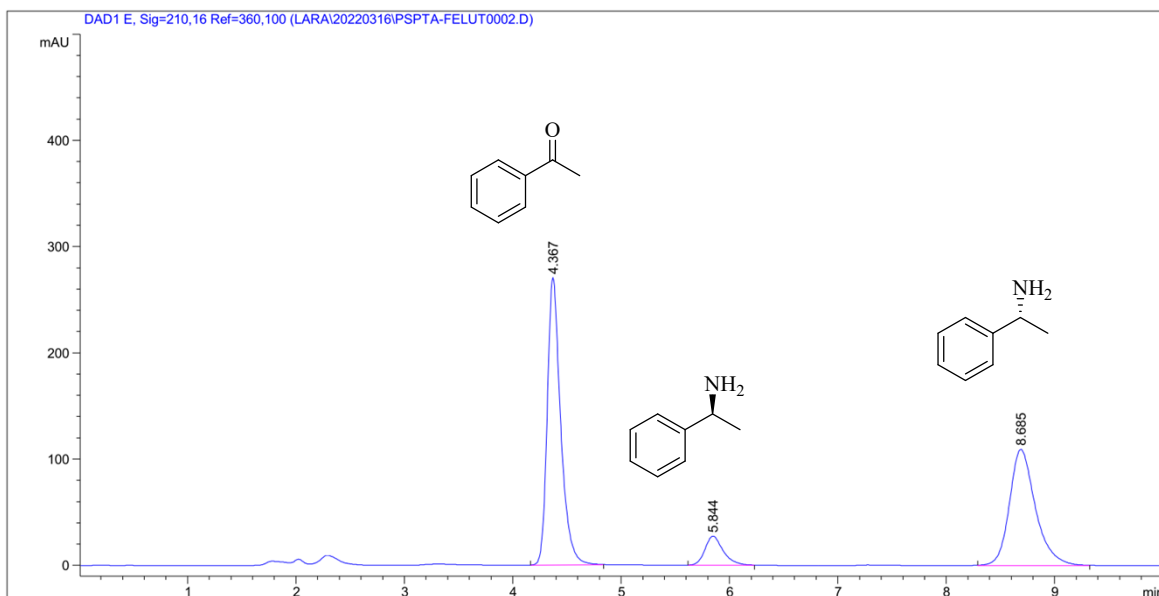


Fig. S7. Elution diagram on Crownpak CR-I(+) column of components in the *PpS*-TA-cells-catalyzed KR of (\pm)-**1a** (100 mM) after 30 min of reaction time

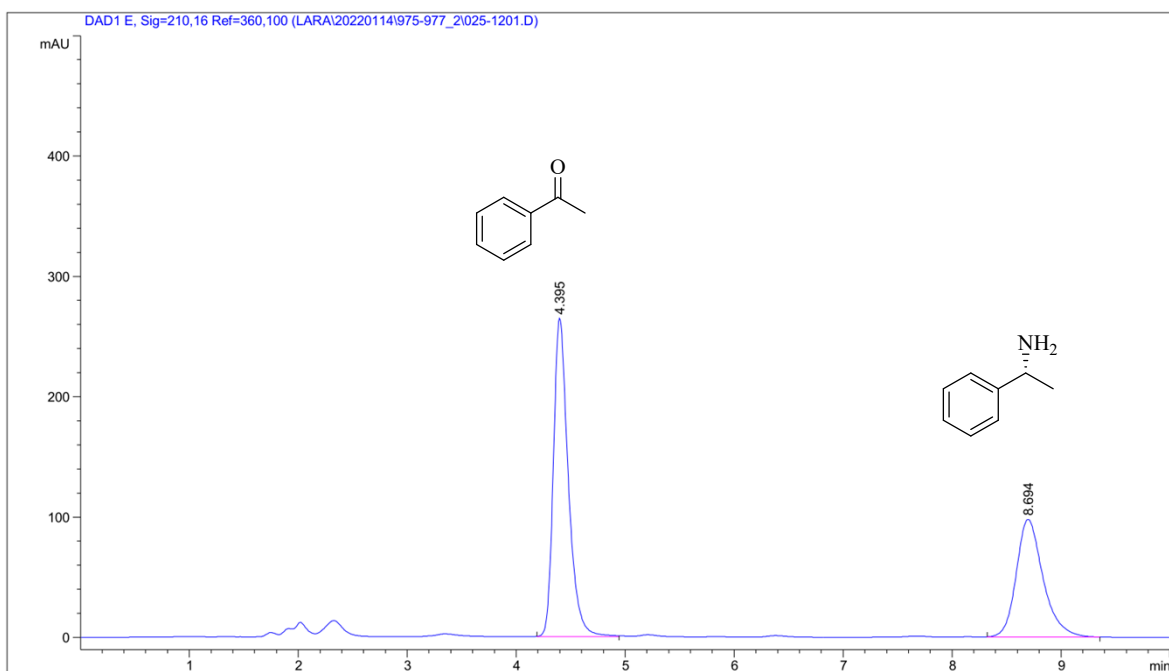


Fig. S8. Elution diagram on Crownpak CR-I(+) column of products in the *PpS*-TA-cells-catalyzed KR of (\pm)-**1a** (100 mM) at the end of the reaction

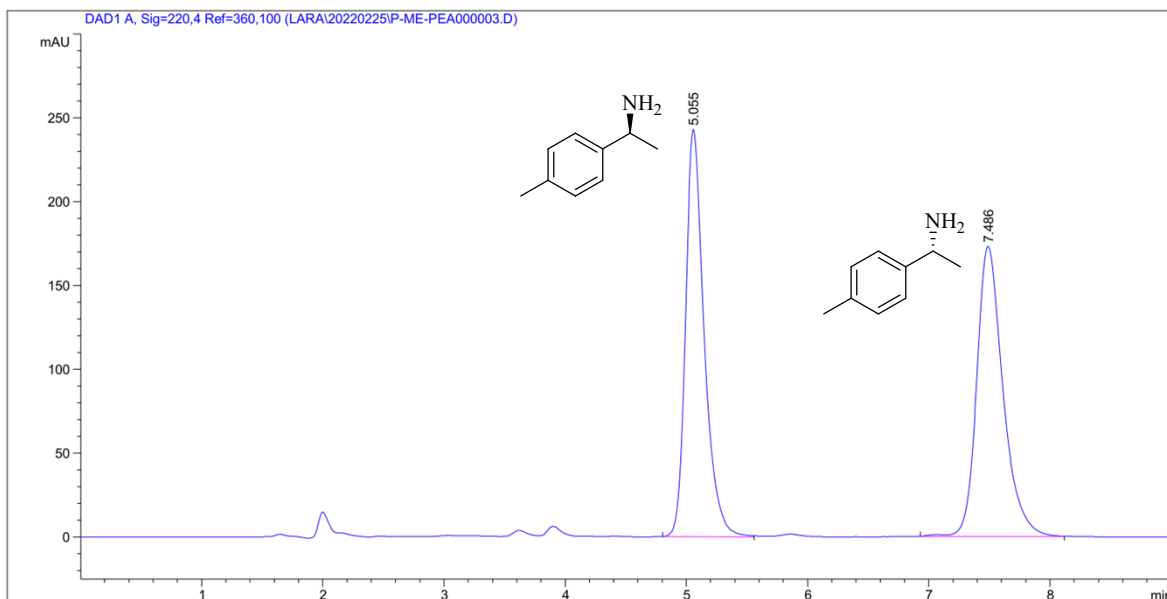


Fig. S9. Chiral separation of (±)-**1b** on Crownpak CR-I(+) column

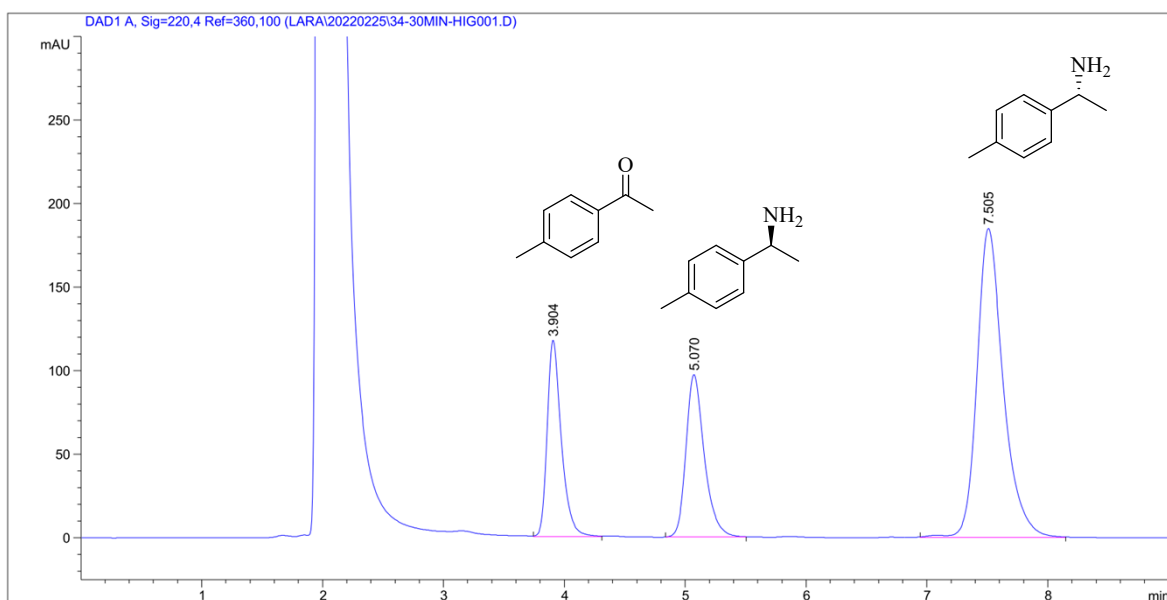


Fig. S10. Elution diagram on Crownpak CR-I(+) column of components in the *PpS*-TA-cells-catalyzed KR of (±)-**1b** (100 mM) after 30 min of reaction time

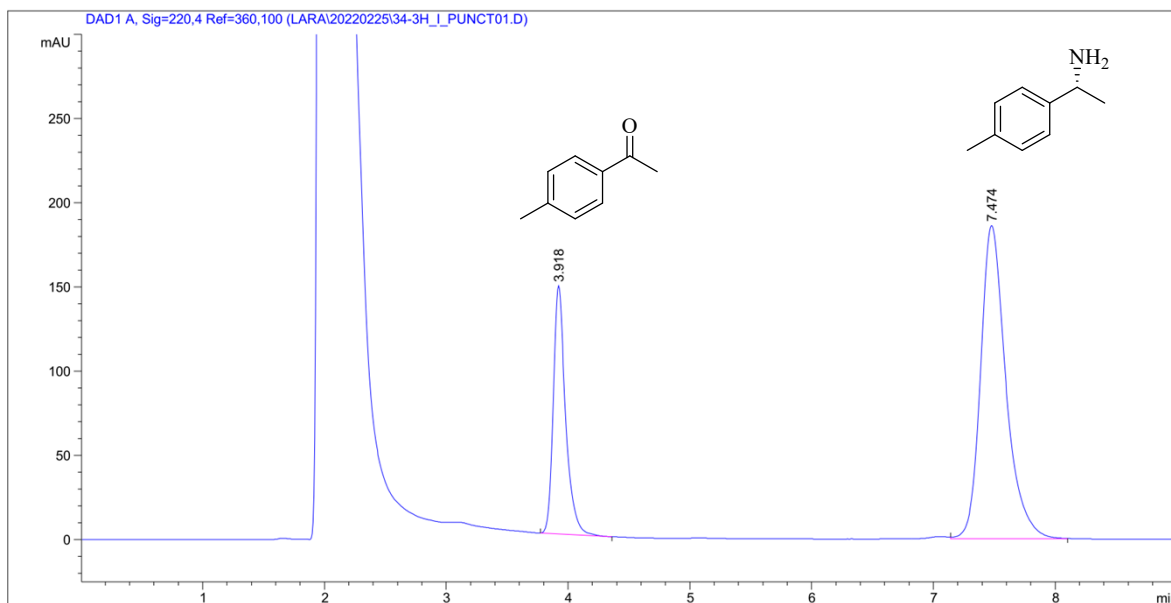


Fig. S11. Elution diagram on Crownpak CR-I(+) column of products in the *PpS*-TA-cells-catalyzed KR of (±)-**1b** (100 mM) at the end of the reaction

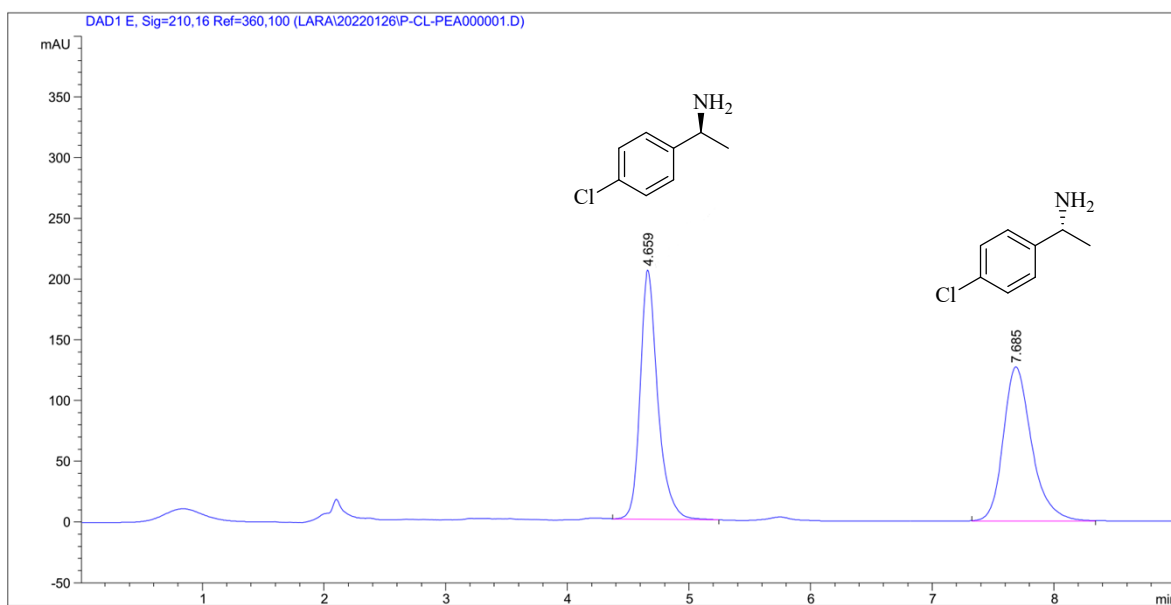


Fig. S12. Chiral separation of (±)-**1c** on Crownpak CR-I(+) column

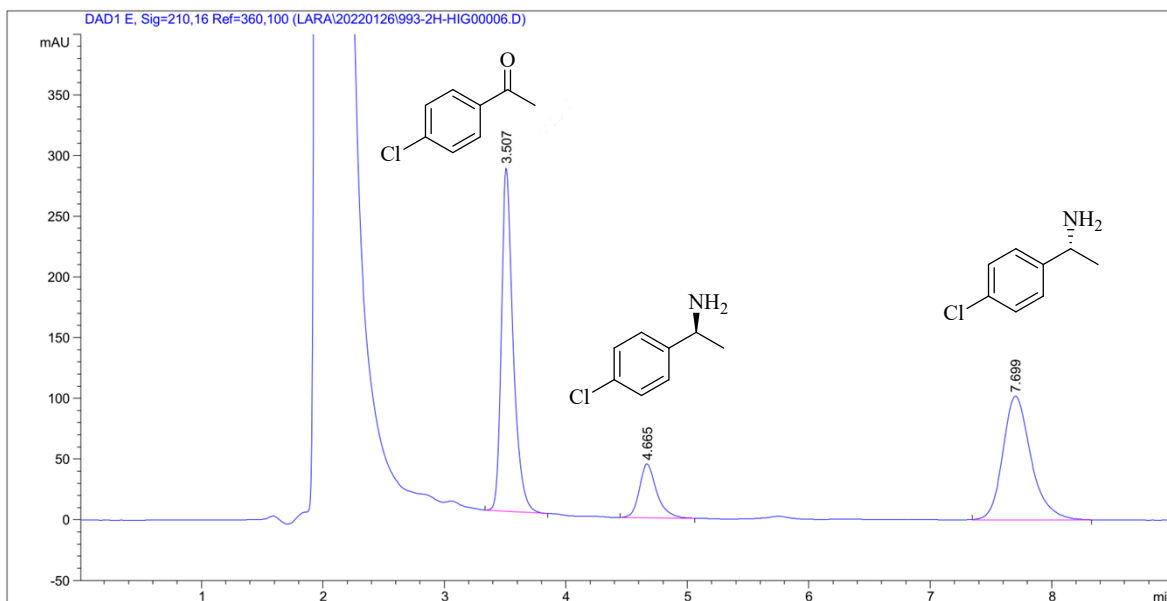


Fig. S13. Elution diagram on Crownpak CR-I(+) column of components in the *PpS*-TA-cells-catalyzed KR of (\pm)-**1c** (10 mM) after 2 hours of reaction time

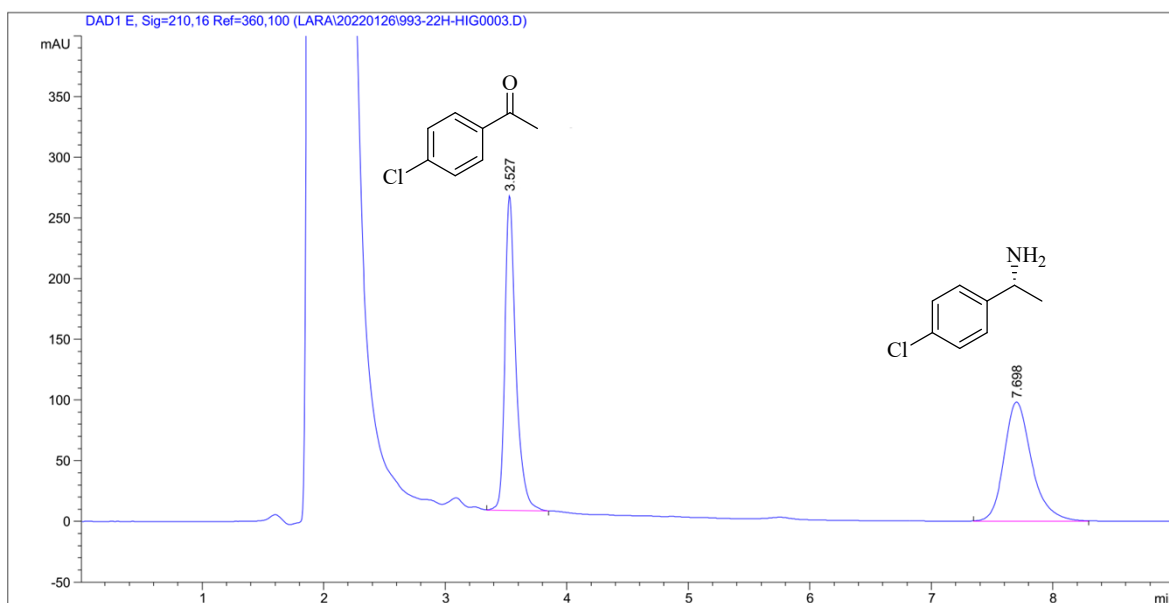


Fig. S14. Elution diagram on Crownpak CR-I(+) column of products in the *PpS*-TA-cells-catalyzed KR of (\pm)-**1c** at the end of the reaction

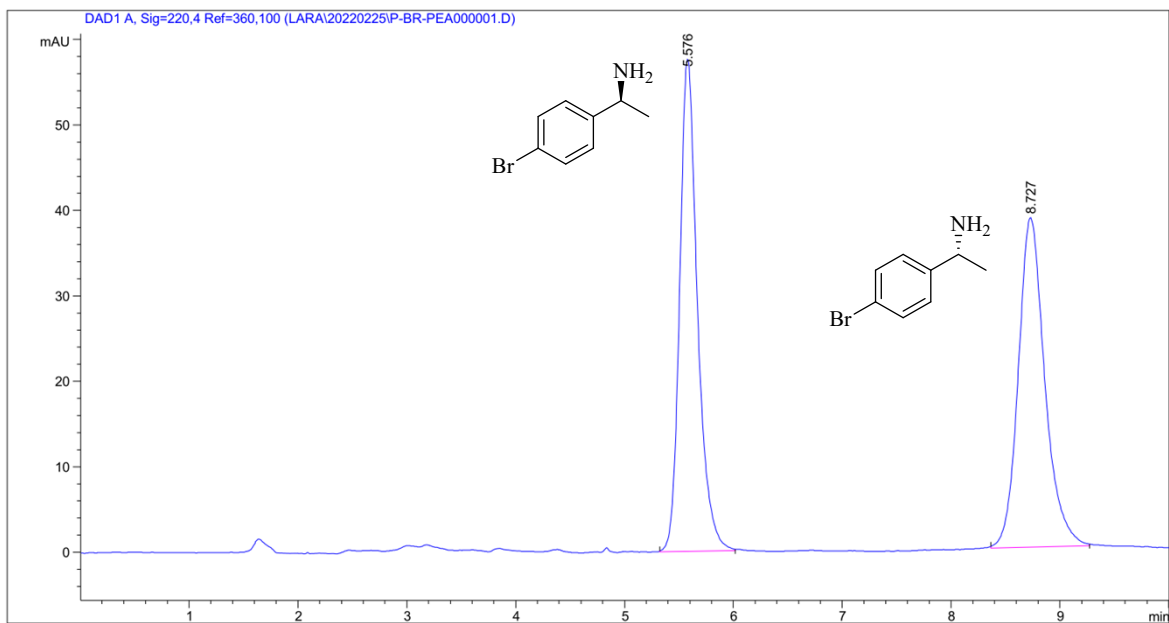


Fig. S15. Chiral separation of (\pm)-**1d** on Crownpak CR-I(+) column

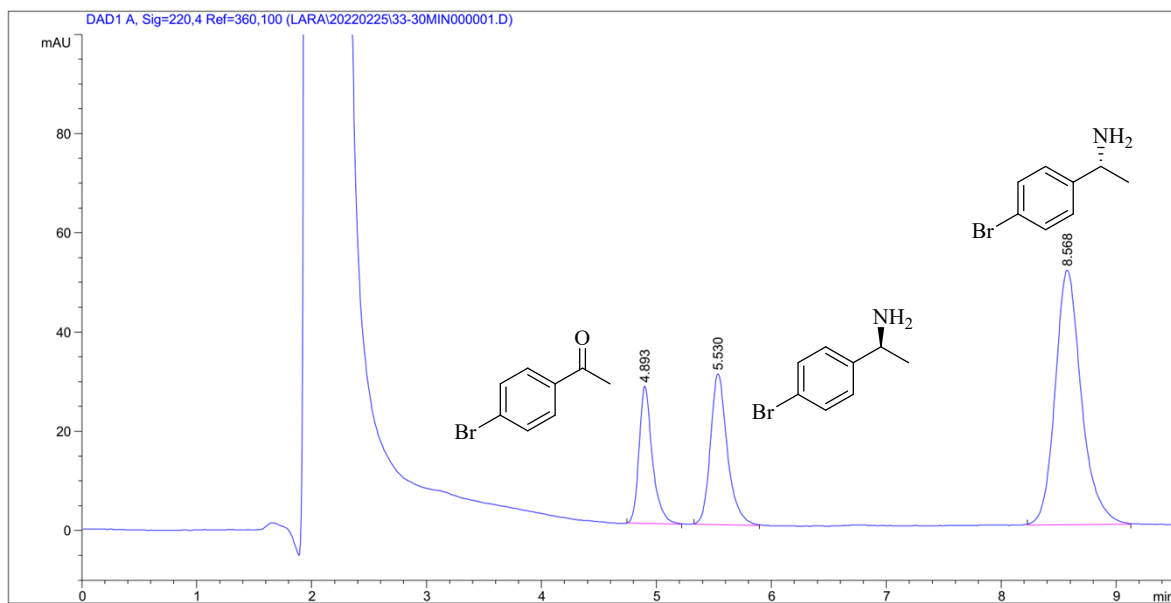


Fig. S16. Elution diagram on Crownpak CR-I(+) column of components in the *PpS*-TA-cells-catalyzed KR of (\pm)-**1d** (5 mM) after 30 min of reaction time

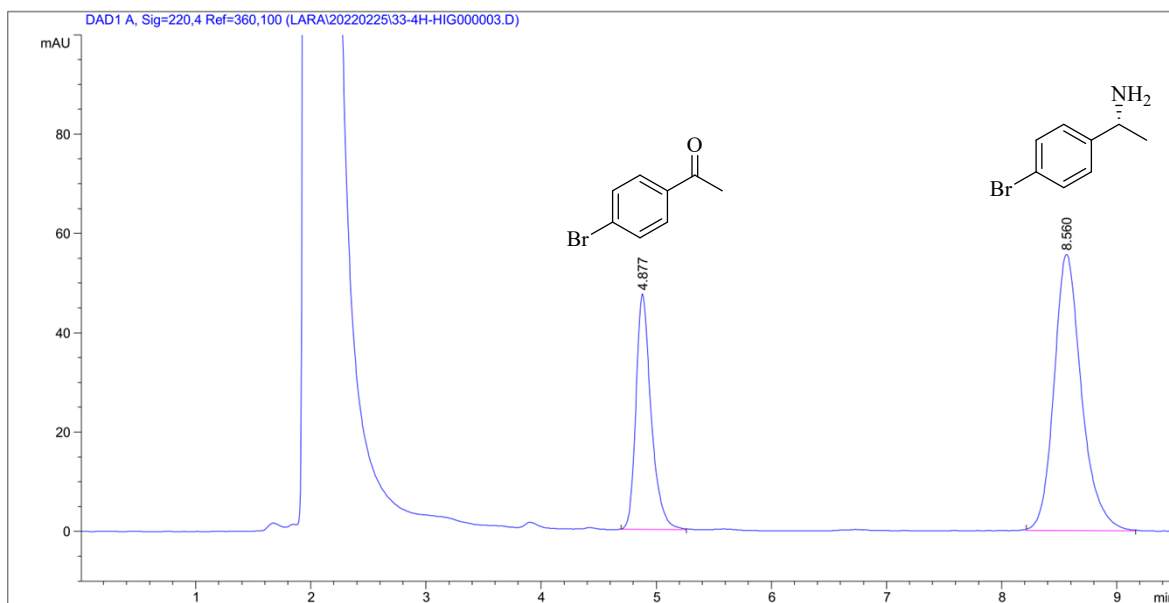


Fig. S17. Elution diagram on Crownpak CR-I(+) column of products in the *PpS*-TA-cells-catalyzed KR of (\pm)-**1d** at the end of the reaction

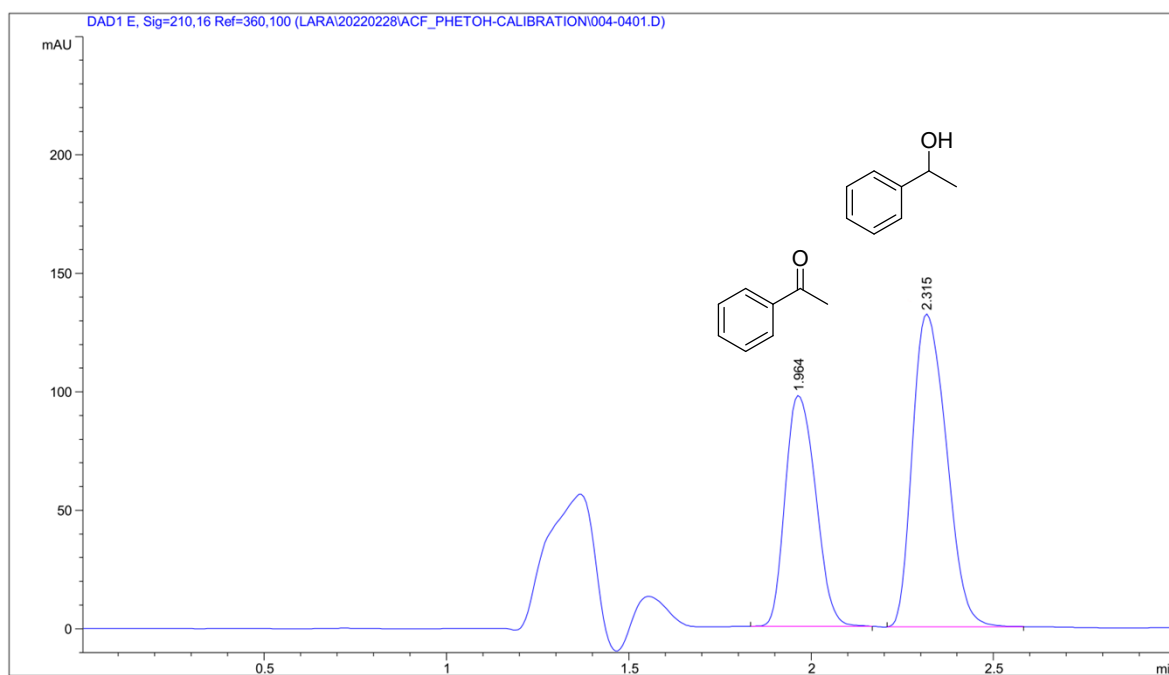


Fig. S18. Separation of the reaction counterparts in the hCAII-catalyzed reduction of the **2a** on ZORBAX Eclipse XDB-C8 column

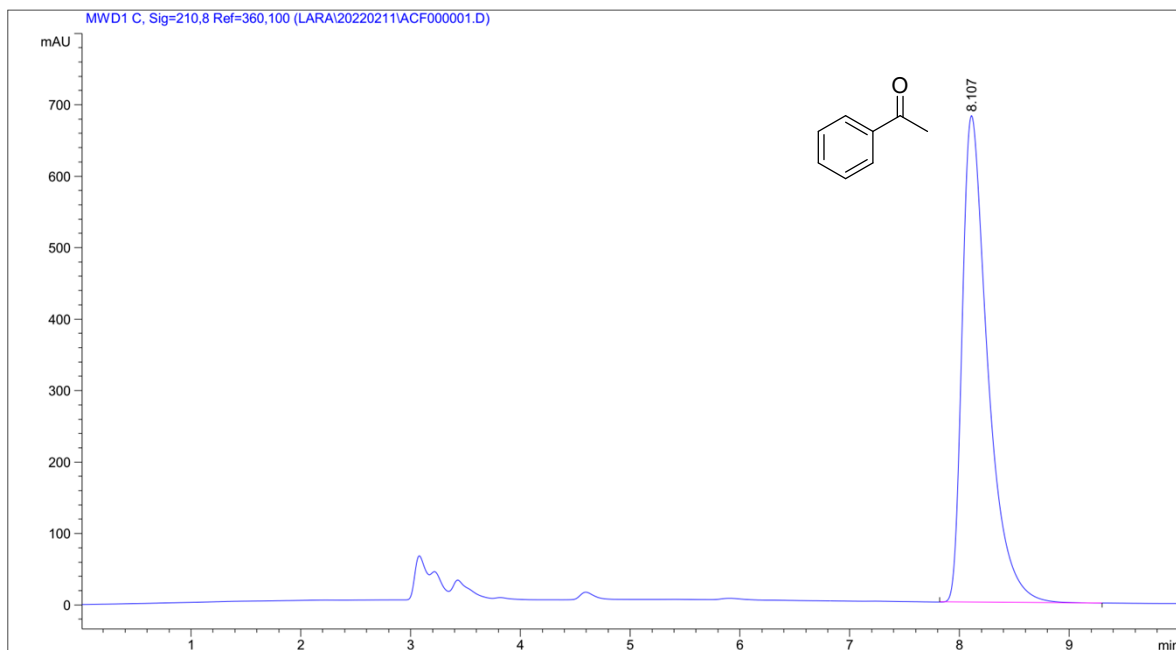


Fig. S19. HPLC chromatogram of **2a** on CHIRALPAK AS-H column

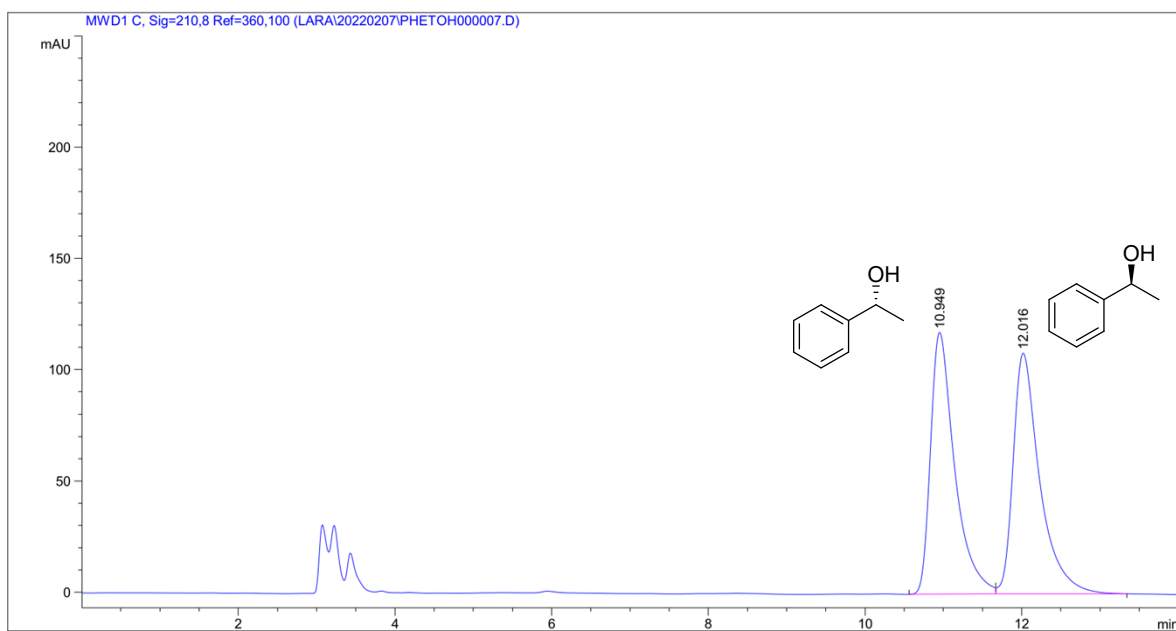


Fig. S20. Chiral separation of (\pm)-**3a** on CHIRALPAK AS-H column

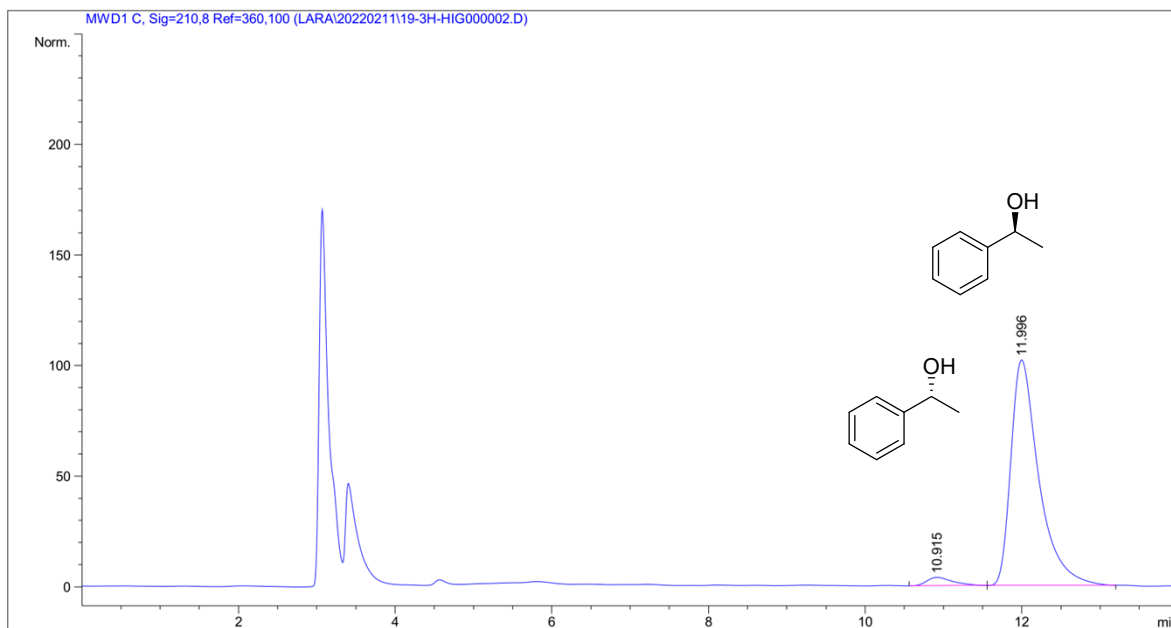


Fig. S21. Enantiomeric composition of (S)-**3a** formed in the hCAII-mediated reduction of **2a**

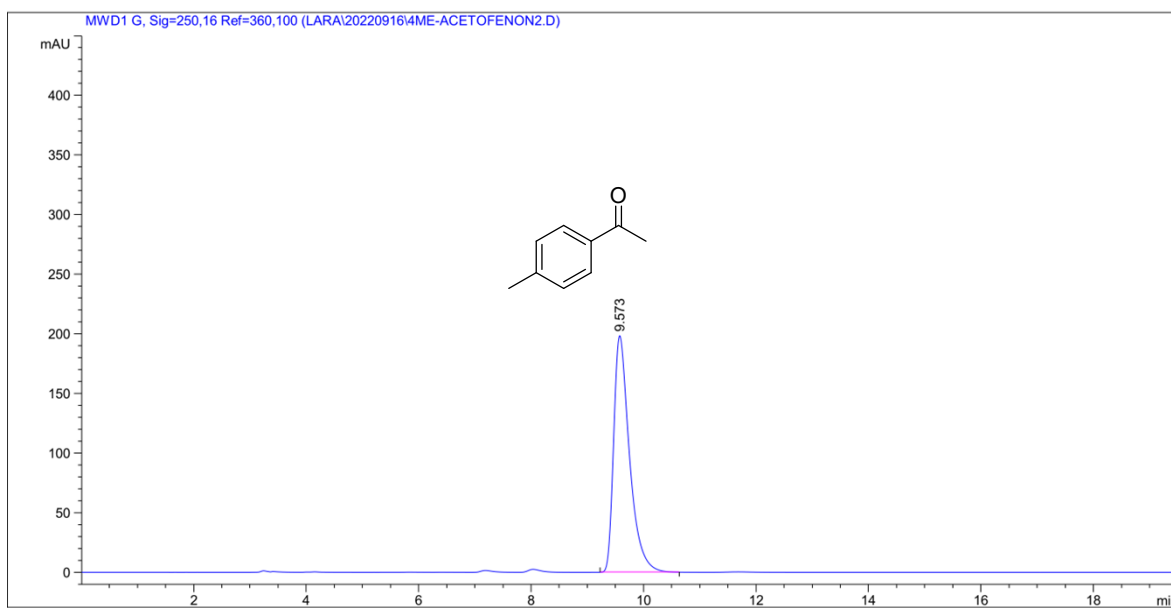


Fig. S22. HPLC chromatogram of **2b** on CHIRALPAK AS-H column

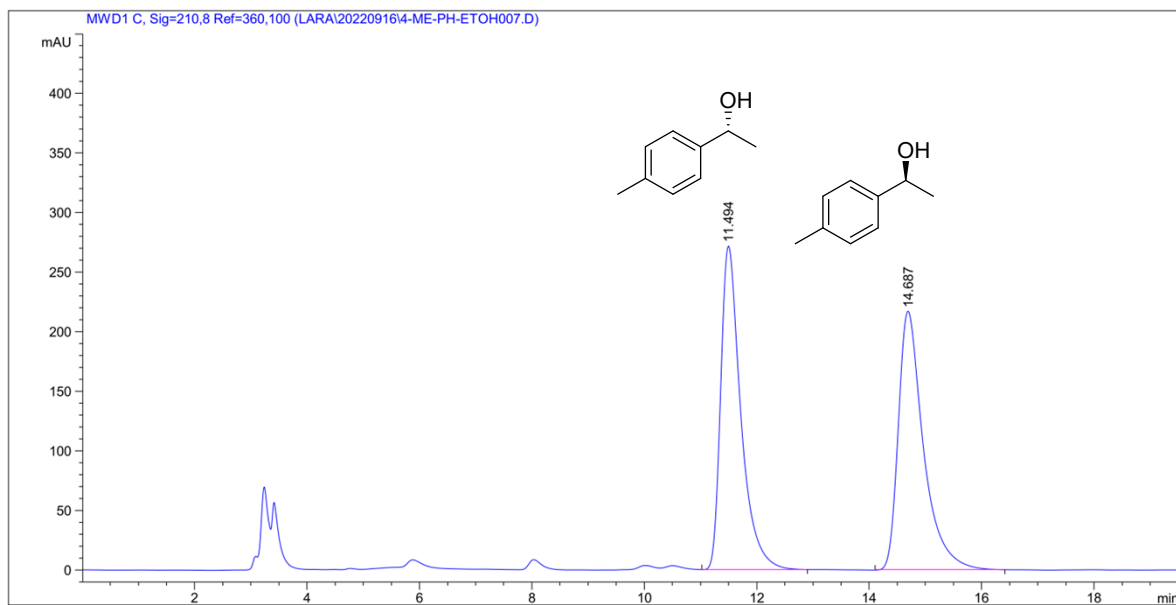


Fig. S23. Chiral separation of (±)-**3b** on CHIRALPAK AS-H column

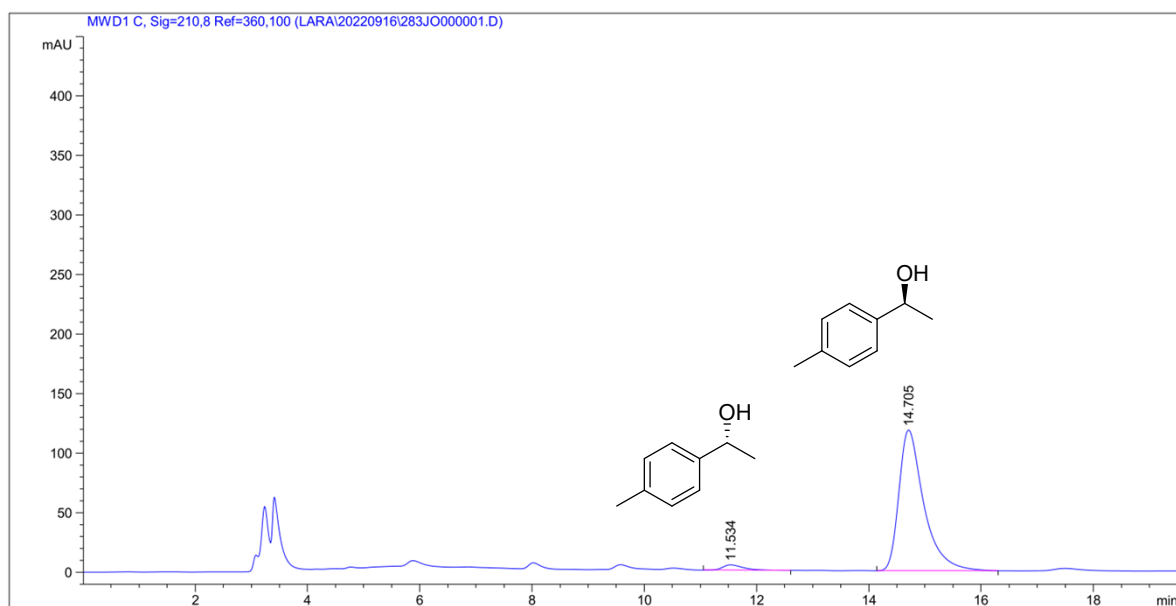


Fig. S24. Enantiomeric composition of (S)-**3b** formed in the hCAII-mediated reduction of **2b**

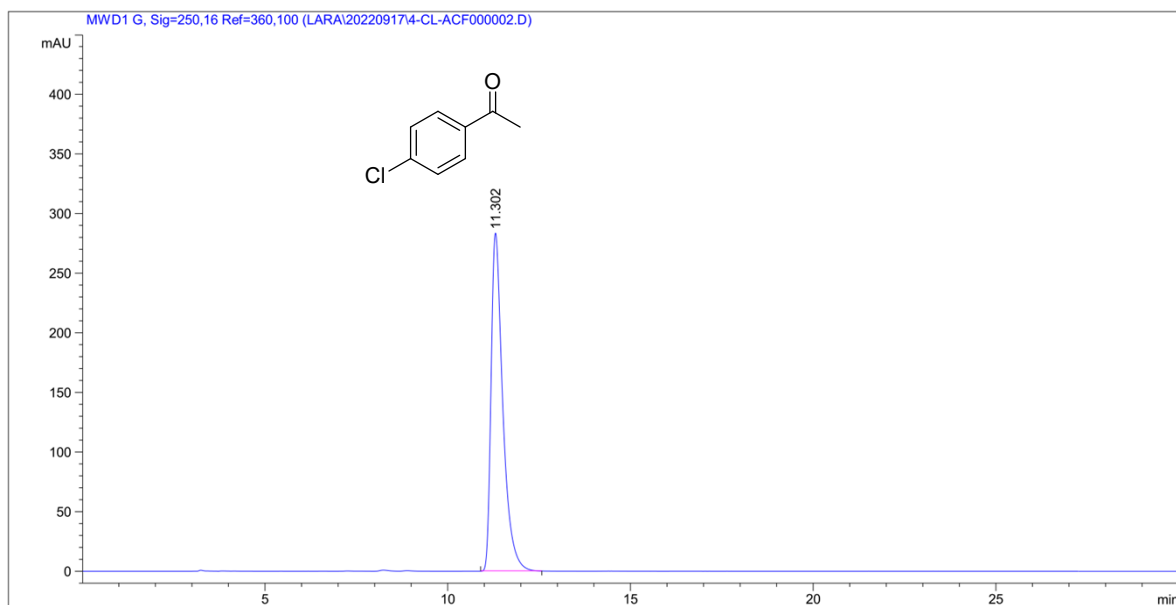


Fig. S25. HPLC chromatogram of **2c** on CHIRALPAK AS-H column

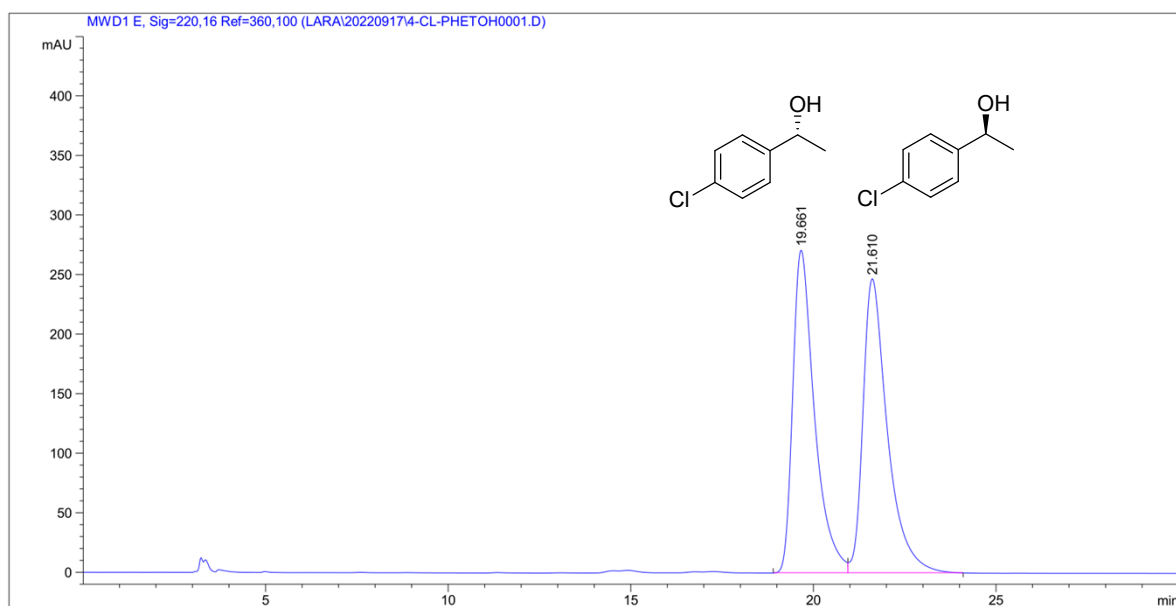


Fig. S26. Chiral separation of (\pm)-**3c** on CHIRALPAK AS-H column

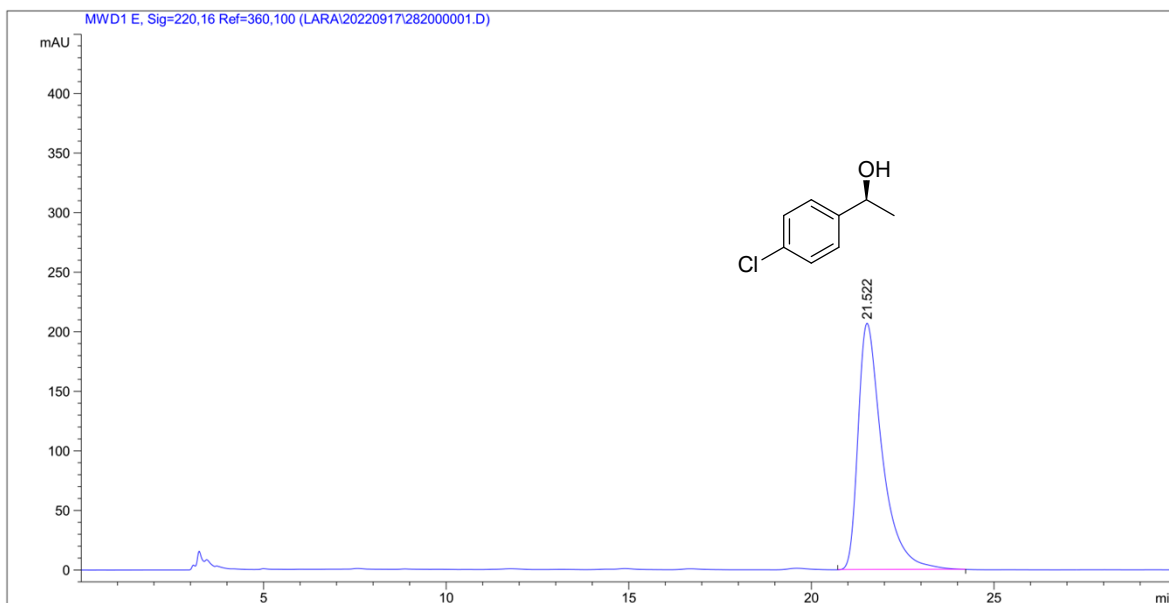


Fig. S27. Enantiomeric composition of (*S*)-**3c** formed in the hCAII-mediated reduction of **2c**

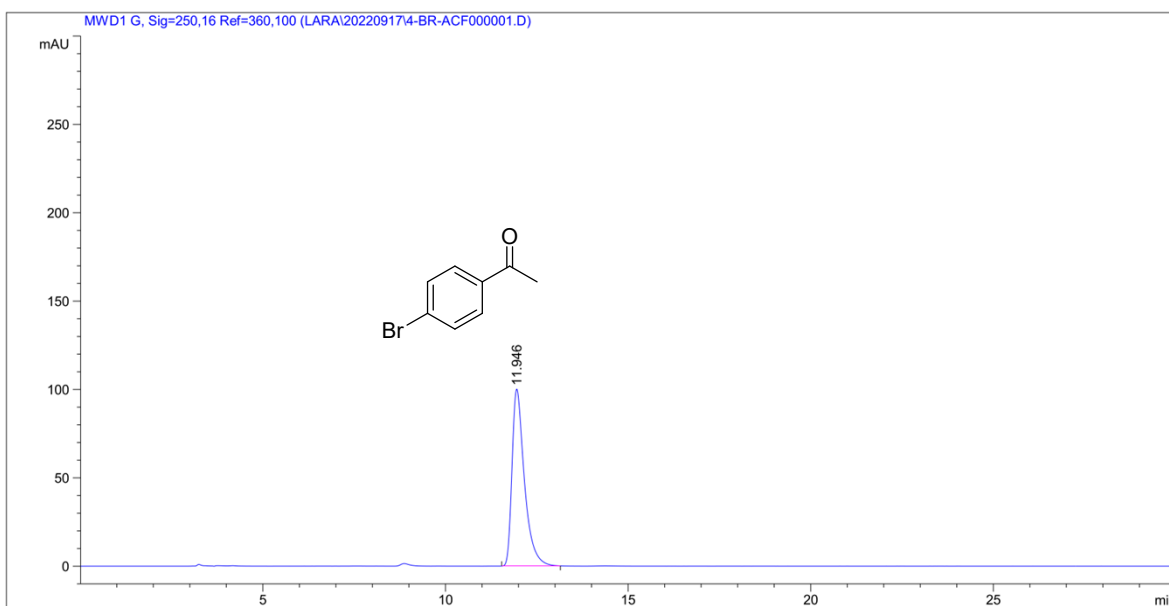


Fig. S28. HPLC chromatogram of **2d** on CHIRALPAK AS-H column

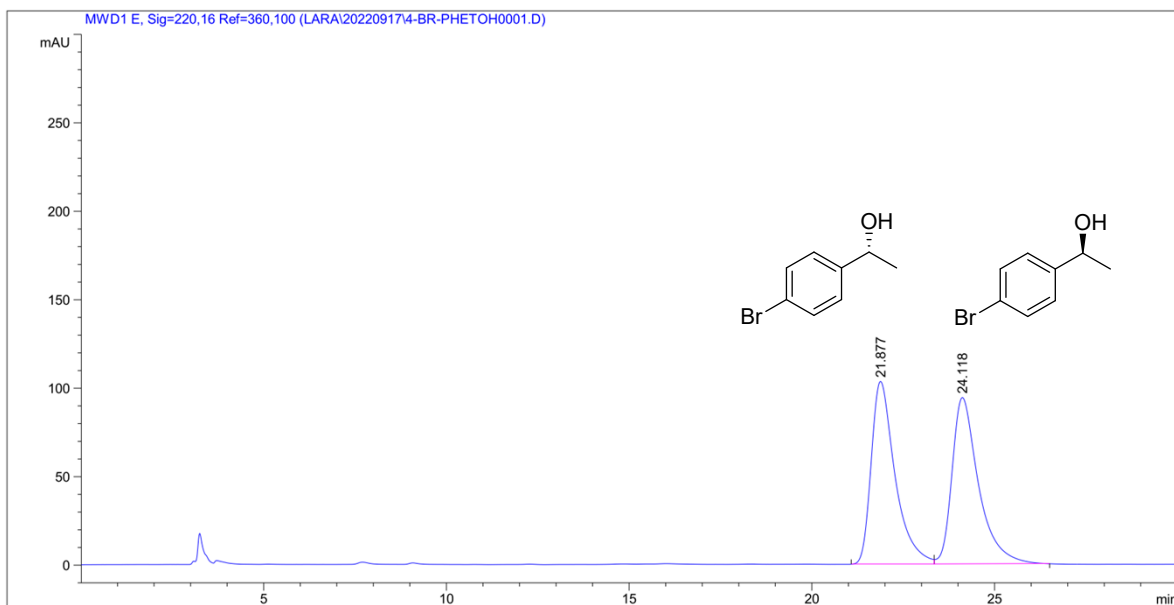


Fig. S29. Chiral separation of (±)-**3d** on CHIRALPAK AS-H column

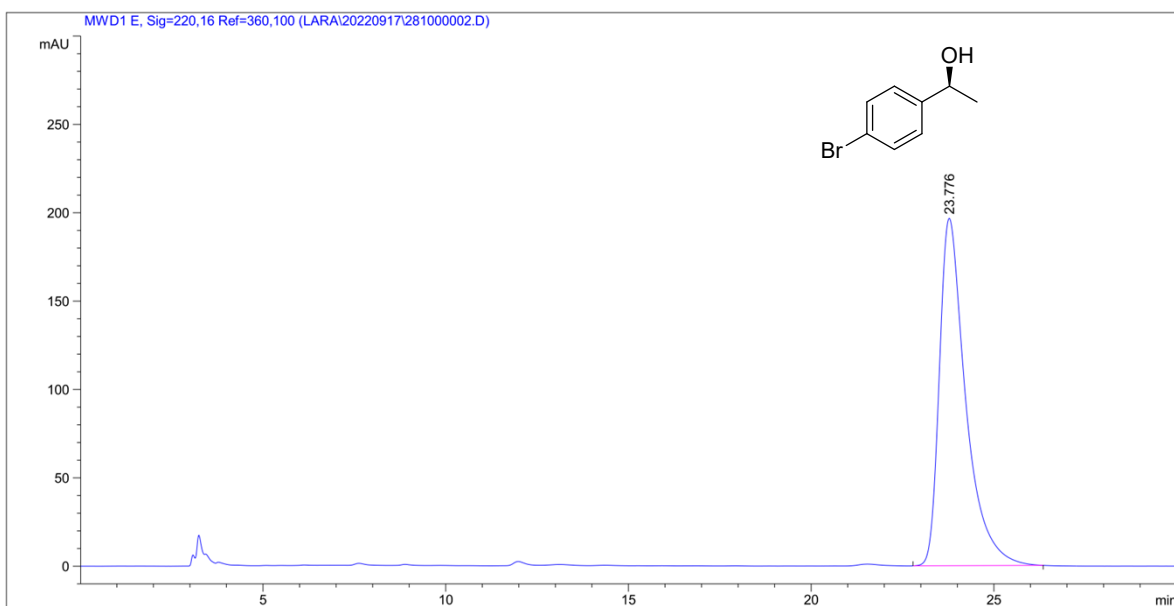


Fig. S30. Enantiomeric composition of (S)-**3d** formed in the hCAII-mediated reduction of **2d**

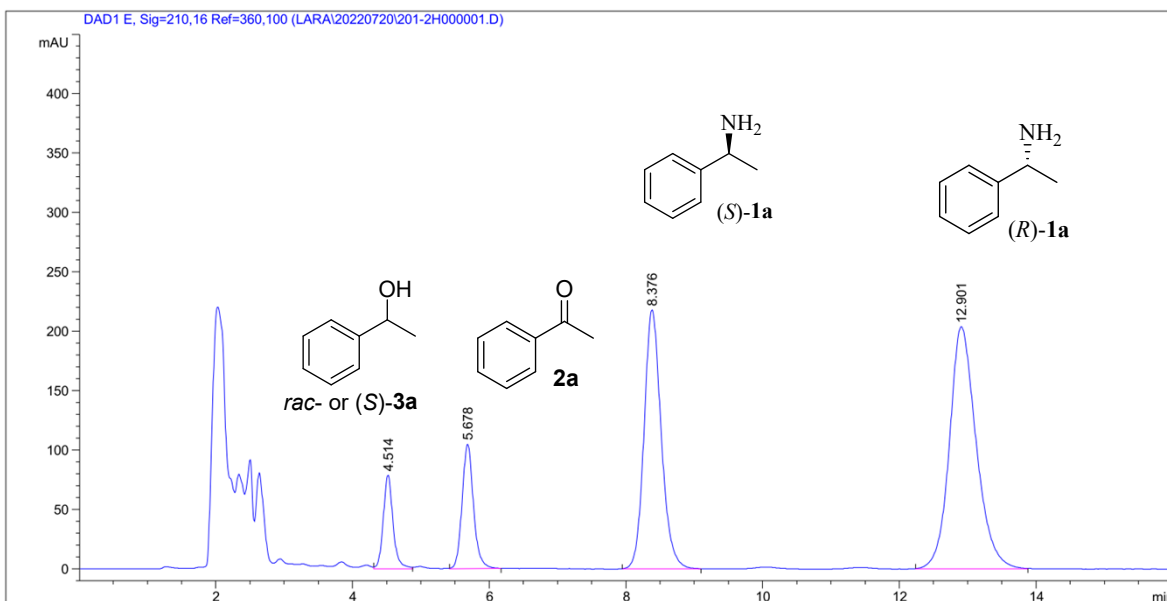


Fig. S31. Elution diagram on Crownpak CR-I(+) analytical column of the authentic components of the bi-enzymatic cascade (KR of (\pm)-**1a** mediated by *Pps*-TA-cells followed by the hCAII-cells-mediated reduction of **2a** formed in the first stage)

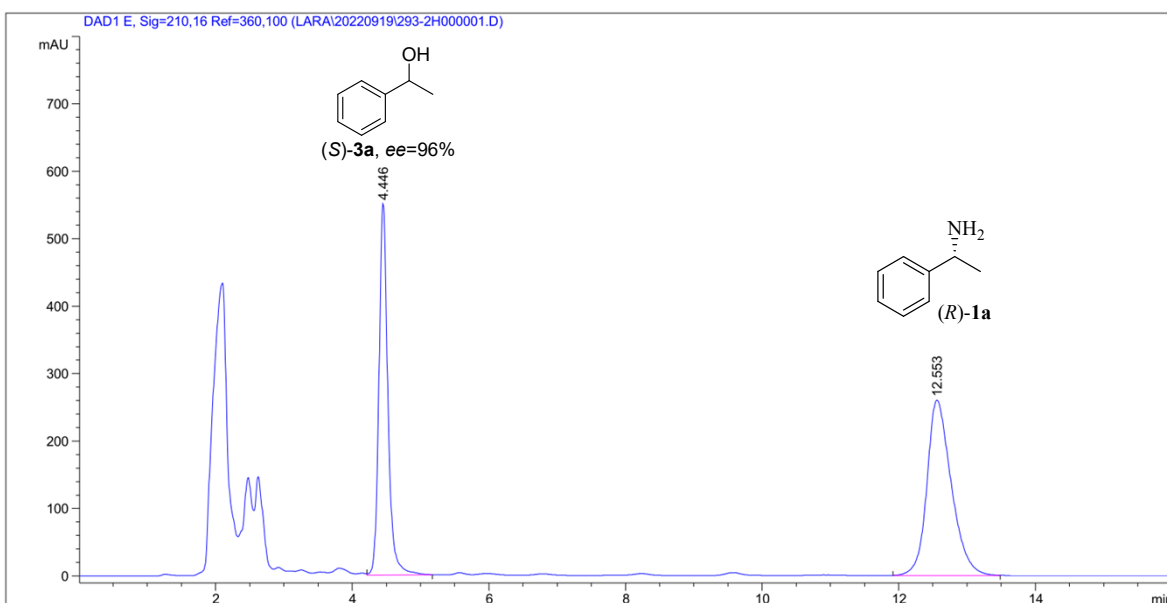


Fig. S32. Elution diagram on Crownpak CR-I(+) analytical column of preparative *Pps*-TA-cell / hCAII-cell cascade's products. The ee for (*S*)-**3a** was determined as shown in Fig. S20 and Fig. S21

S8. Effect of cosolvent content on the catalytic performance of hCAII

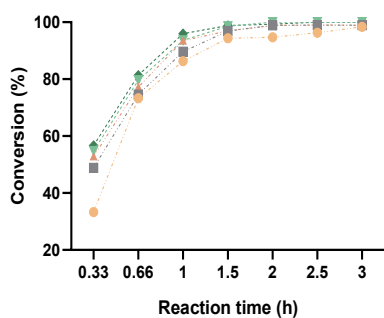


Fig. S33. Activity of the biocatalyst in absence of DMSO in the enzymatic reduction of **2a** catalyzed by hCAII

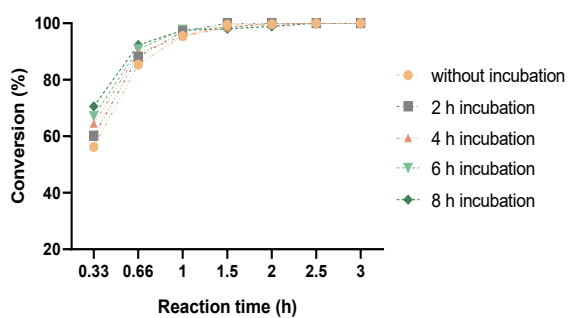


Fig. S34. Activity of the biocatalyst in the presence of 10 % DMSO (v/v) in the enzymatic reduction of **2a** catalyzed by hCAII

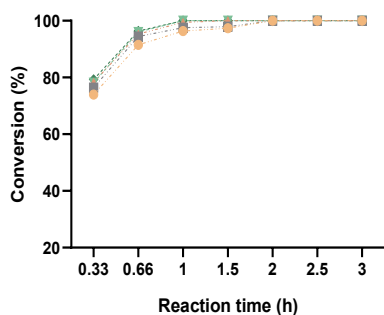


Fig. S35. Activity of the biocatalyst in the presence of 20 % DMSO (v/v) in the enzymatic reduction of **2a** catalyzed by hCAII

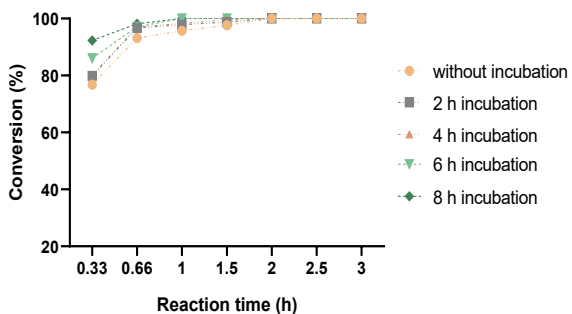


Fig. S36. Activity of the biocatalyst in the presence of 30 % DMSO (v/v) in the enzymatic reduction of **2a** catalyzed by hCAII

S9. Cellular biotransformation

Table S3. Influence of the biocatalyst loading on the conversions of *PpS*-TA-cells-catalyzed KR of (\pm)-**1a**

Lyophilized cell powder (mg mL ⁻¹)	Conversion (%)
2.5	21.6
5	29.4
10	36.6
20	45.6
30	~50

KR of (\pm)-**1a** in PB buffer (100 mM, pH 7.0), 100 mM substrate concentration, 100 mM cosubstrate, 0.1 mM PLP.

Table S4. Conversions of the *PpS*-TA-cells-mediated reaction at different (\pm)-**1a** concentrations after 8 hours reaction time

Substrate concentration (mM)	Conversion (%)
90	~50
100	~50
110	43.6
120	34
130	30.8

Reaction conditions: phosphate buffer solution (PB, 100 mM, pH 7.0), stoichiometric equivalent of sodium pyruvate, 25 mg mL⁻¹ lyophilized *PpS*-TA-cell powder, 0.1 mM PLP.

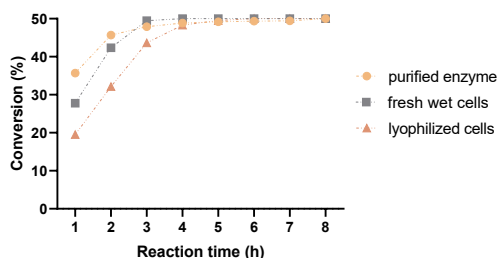


Fig. S37. Kinetic resolution of 40 mM **1a** mediated by *PpS*-TA (purified enzyme, fresh wet *E. coli* cells with intracellularly overexpressed enzyme, lyophilized *E. coli* cells with intracellularly overexpressed enzyme - containing the same amount of enzyme ~100 μ g mL⁻¹) at 40 °C^a

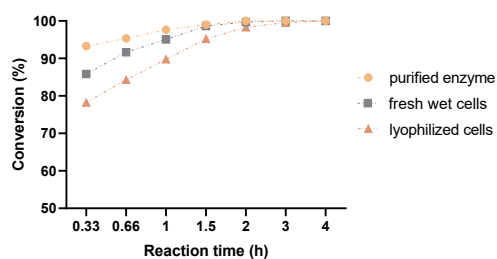


Fig. S38. Enzymatic reduction of 50 mM **2a** mediated by hCAII (purified enzyme, fresh wet *E. coli* cells with intracellularly overexpressed enzyme, lyophilized *E. coli* cells with intracellularly overexpressed enzyme - containing the same amount of enzyme) at 20 °C in the presence of 30 % DMSO and 3 equiv. phenylsilane^a

^aAfter completion of the enzyme production process, the cell suspension was divided into three parts. After centrifugation, one third was purified by Ni-NTA affinity chromatography, the second third was used for the reactions after resuspension in the buffer solution, and the third third was freeze-dried. After determining the protein concentration, a sufficient amount of the wet and lyophilized cells containing the amount of enzyme corresponding to the purified dissolved enzyme was used for the reactions.